Ω
SPE 30560

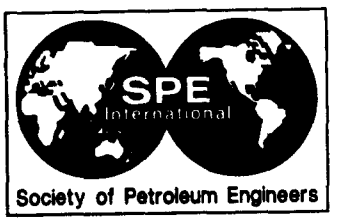

Processing of Data From an NMR Logging Tool

R. Freedman, SPE and C.E. Morriss, SPE, Schlumberger Wireline & Testing

This paper was prepared for presentation at the SPE Annual Technical Conference & Exhibition held in Dallas, U.S.A., 22-25 October, 1995.

Abstract

A new pulsed nuclear magnetic resonance (NMR) logging tool, known as the CMR* Combinable Magnetic Resonance tool, is being used worldwide. During the CMR tool development phase, one challenge was to design a robust and economical data acquisition and signal processing scheme for the hundreds or thousands of spin-echo amplitudes that can be acquired during the Carr-Purcell-Meiboom-Gill (CPMG) pulse sequence. This challenge was met by developing a new signal processing and associated downhole data compression algorithm. Data compression is essential to reducing the processing times so that formation T2-distributions can be estimated in real time. Compression of the digital data is possible, without loss of information, because the linear dependency of the NMR measurement kernels results in gross redundancy of the measured spin-echo amplitudes.

An attractive feature of the algorithm described in this paper is that the compression can be performed in the downhole tool, thus substantially reducing the telemetry requirements. The raw spin echoes can also be sent uphole and made available for additional processing.

Logs of CMR porosity, free-fluid porosity, mean relaxation time and rock permeability are computed from the estimated T2-distributions. The accuracy and precision of the CMR log outputs are demonstrated by repetitive Monte Carlo computer simulations in which noisy, synthetic spin-echo amplitudes are generated from known T2-distributions and then processed to obtain log outputs. Monte Carlo simulations are used to elucidate CMR log responses in typical clean sand, shaly sand, and carbonate rocks. The relative insensitivity of the measurements to short relaxation times (e.g., those less than a few milliseconds) is discussed and used to explain the differences between CMR log porosity and "total" formation porosity in shaly formations. We show that CMR porosity is an "effective porosity" that does not include clay bound water and microporosity having relaxation times less than a few milliseconds.

We give examples of statistical fluctuations that can occur on estimated T2-distributions to assist log analysts in recognizing artifacts that are not indicative of actual reservoir rock properties. Field logs that display many of the features of CMR log responses revealed by the simulations are also presented.

Introduction

The physics underlying pulsed NMR has been known since 1950.[1] Pulsed NMR has been used since its discovery as a probe for studying the macroscopic and microscopic properties of condensed matter. Its original applications were in industrial and academic laboratories. More recently, magnetic resonance imaging has become a powerful nonradioactive diagnostic tool for medical research and clinical applications.

The recent development of pulsed NMR well logging tools[2,3] had to await the development of new technology, e.g., integrated circuits, microprocessors, and stable high-field permanent magnets. The CMR tool is a product of these technological advances and years of research[4] and development effort. The CMR tool is a pad-type tool that performs pulsed NMR measurements using Carr-Purcell-Meiboom-Gill (CPMG) pulse sequences. The spin-echo signals acquired during the measurement are derived from protons (i.e., hydrogen nuclei) that precess in the static magnetic field produced by a permanent magnet in the sonde. The protons are contained in the fluids that occupy the rock pore spaces.

A CPMG consists of two time intervals: (1) an initial wait time during which the proton magnetization approaches its thermal equilibrium value in the static magnetic field and (2) the echo collection period during which a set of radio frequency (RF) pulses generated by an antenna in the sonde are used to generate the spin echoes. The nominal tool inter-echo spacing is 0.32 ms. The wait time interval normally accounts for most of the CPMG measurement time. The CPMG spin-echo sequences are

* Mark of Schlumberger

acquired as phase-alternated pairs (PAPs) in order to cancel baseline offsets. The same antenna that generates the RF pulses is also used to receive the nanovolt level spin-echo signals from the formation. The antenna has a uniform response over its 6-in. [15.24-cm] length which accounts for the high vertical resolution of the CMR measurements. The CMR response has a blind zone of approximately 0.5 in. [1.27 cm] which provides immunity to mudcake and moderate borehole rugosity effects. The measured integrated radial response of the CMR tool shows that 90 percent of the signal is derived from within 1.3 in. [3.3 cm] of the borehole wall.

A spin-echo sequence with 600 echoes is shown in Fig. 1. The signal-to-noise-ratio (SNR) of the data shown in this example is in the midrange of that typically acquired during CMR depth logging operations.

T2-Distributions. The decay of spin-echo sequences in porous rocks are properly described by continuous T2-distributions.[5,6] The multi-exponential nature of NMR relaxation in rocks is a result of the pore size distribution. That is, under some plausible assumptions, it can be shown that the T2-decay rate of NMR signals from fluids in an individual pore is proportional to its surface-to-volume ratio. The total NMR signal (being the superposition of signals from a distribution of individual pores) is therefore a summation of single exponential decays. The sum of the amplitudes of the individual decays is proportional to the total porosity measured by the tool.

T2-distributions are displayed by plotting the amplitudes versus their associated relaxation times on a logarithmic scale. The computed T2-distributions are the primary result of the processing and are used to compute logs of CMR porosities (ϕ_{cmr}), free-fluid porosities (ϕ_{ff}), capillary bound fluid porosities (ϕ_{bf}) and logarithmic mean relaxation times ($T_{2,log}$).

A T2-distribution typical of a clean sandstone formation is shown in Fig. 2. The total porosity is proportional to the area under the T2-distribution. The free-fluid porosity is proportional to the shaded area having T2 relaxation times greater than 33 ms. The 33 ms is an empirically determined cutoff that is frequently used in sandstones to partition the distribution into bound and free-fluid porosities.[2] The logarithmic mean relaxation time for the distribution is 44 ms. The logarithmic mean relaxation time of a distribution is analogous to the "center of mass" of a body in classical mechanics. The logarithm of the mean relaxation time is computed by averaging the logarithms of the relaxation times in the distribution each weighted by its signal amplitude. The logarithmic mean relaxation times are used in the estimation of permeability in sandstone formations.

Processing Challenges

As noted above, many unique hardware and software problems associated with the borehole environment had to be confronted and solved. The development of an optimal real-time signal processing algorithm for NMR well logging data was one of the problems. The main requirements of the processing are: (1) to provide accurate and robust logs, (2) to provide real-time logs with the computer resources available at the wellsite and (3) to provide operational flexibility for a tool capable of operating in different modes. The following constraints made satisfying these requirements a significant technical challenge.

High Data Rate Measurements. In standard depth logging modes, 600 or 1200 spin-echo amplitudes are typically recorded in each of two channels using quadrature detection. During station logging, as many as 8000 spin echoes are acquired. The two channel data are used to estimate the phase of the signal and combine the two channels into: (1) a phase coherent channel that contains the total signal amplitude plus noise (hereafter called the "signal channel") and (2) a channel that contains only noise (hereafter called the "noise channel"). The data in the signal channel are used to compute T2-distributions. The data in the noise channel are used to estimate the root-mean-square (RMS) noise. The RMS noise is used as discussed in a later section to compute the standard deviations in the CMR logs.

Signal-to-Noise Ratios. The SNR of borehole NMR measurements is substantially lower than that of data acquired by most other well logging tools. For the CMR tool each echo in a PAP contains zero mean Gaussian noise with RMS amplitude equal to approximately 3.5 porosity units (p.u.).

During depth logging, a three-level averaging of PAPs is normally performed prior to processing the data. Three level averaging reduces the RMS noise on each spin echo to about 2.0 p.u. Therefore, the SNR of the data typically processed during depth logging ranges from 15 to about 2 in reservoir quality rocks. Unfortunately, the SNR decreases with increasing borehole and formation temperatures due to two effects. First, the tool thermal noise increases with borehole temperature. Secondly, the measured spin-echo amplitudes decrease with increasing formation temperature according to the well-known Curie law of paramagnetism.

Ill-Posed Inversion Problem. The computation of T2-distributions from spin-echo sequences involves a mathematical inverse problem. The inverse problem is the estimation of the amplitudes in the multi-exponential model (e.g., 30 components are typically used during depth logging) from the noisy spin-echo data.

NMR data from rocks can be adequately fit to a simple relaxation model involving a few exponentials or to a stretched exponential model. These simple models are

mathematically stable but do not provide valuable information on pore size distribution and free fluid that is contained in the T2-distributions.

The inverse problem that must be confronted in computing T2-distributions is mathematically ill-posed. It can be shown that a spin-echo sequence consisting of hundreds or thousands of spin-echo amplitudes contains only a few linearly independent pieces of information. That is, the spin-echo data are redundant because of the approximate linear dependency of the NMR measurement kernels. The redundancy can be demonstrated by computing the singular values of the NMR measurement kernel matrix. The redundancy is manifested by the existence of only a few non-zero singular values as shown in Fig. 3. The number of linearly independent data is equal to the number of non-zero singular values. The zero singular values lead to unstable and nonunique solutions to the mathematical inverse problem. The solutions are unstable because arbitrarily small changes in the input data can lead to large changes in the estimated T2-distributions.

Tikhonov Regularization Method. Methods were developed during the 1960's to provide practical solutions to ill-posed inverse problems.[7,8] The regularization method imposes a criterion for selecting a smooth T2-distribution from the possible solutions that are consistent with the data. The smoothness criterion is consistent with the fact that the NMR measurement kernels attenuate the high-frequency components in the underlying T2-distributions. That is, NMR data intrinsically have low frequency content, which is the rationale for selection of a smooth distribution. The regularization not only reduces the statistical fluctuations on the computed T2-distributions but it also controls the standard deviations of the logs.

Processing Overview

Data Redundancy and Data Compression. It was realized early in the tool development phase that existing methods of inversion were not well suited for real-time processing of the CMR logging data. In particular, the computation of continuous T2-distributions in real time requires more computer resources than are presently available due to the large quantities of data acquired by the tool. It was also realized that the NMR spin-echo data are grossly redundant in a mathematical sense.[9] Consequently, spin-echo sequences can be compressed into a few numbers without loss of information. Data compression is required to compute T2-distributions in real time with available wellsite computing resources.

The data compression algorithm had to be flexible and compatible with a real-time data acquisition and processing environment. These requirements made conventional compression methods based on singular value or eigenvalue decompositions less desirable, since these methods require central processing unit intensive matrix computations each time the pulse sequence parameters are changed. An alternative, which was considered, is the precomputation and storage of these decompositions; but this reduces operational flexibility. Another factor that discriminated against use of the latter methods was the desire to perform the data compression downhole using a digital signal processing chip in the tool electronics cartridge. This required a fast compression algorithm that could be implemented with DSP chips used in downhole tools. The downhole data compression reduces telemetry capacity requirements and also disk and tape storage. The uncompressed data can also be transmitted uphole and stored on disk if required for later processing.

Window Processing Algorithm. The above considerations led to the development of a new inversion and associated data compression algorithm known as the window processing (WP) algorithm.[9,10] A detailed mathematical derivation of the algorithm is beyond the scope of this paper and will be published elsewhere. Some of the details were summarized in a previous publication.[2] This section provides an overview and discusses some features of the processing that later will be illustrated by examples.

Window Sums. The compressed data, in the WP algorithm, are sums of spin-echo amplitudes over a small number of predetermined time intervals that we refer to as "windows." The compressed data are equivalent to wavelet transform coefficients of the spin-echo sequence.[11] These coefficients contain information on different time scales in the T2-distributions. Figure 4 shows averaged window sums and one-standard-deviation error bars computed from the 600 echoes shown in Fig. 1.

The averaged window sums are simply the average spin-echo amplitudes in the five windows whose boundaries are indicated by the dashed lines in Fig. 1. Because of the thermal noise, the averaged amplitudes are random variables. The RMS noise on the averaged amplitude in each window is reduced, by a factor equal to the square root of the number of echoes in the window. For example, the third window in Fig. 1 contains 100 echoes so that the 2.0 p.u. of RMS noise on each spin echo is reduced to 0.2 p.u. on the averaged amplitude.

Sensitivities of Window Sums. The window sums exhibit varying sensitivities to the different components (T2s) in the underlying T2-distribution that produces an observed CPMG. The sensitivities of the average window sums to the components in the T2-distribution are shown in Fig. 5. The sensitivity curves in Fig. 5 were computed for the five windows shown in Fig. 1 for an inter-echo spacing of 0.32 ms. Note that window sums from later windows have less sensitivity to the shorter T2 components in a distribution than those from the earlier windows. In particular, only the first three window sums show much sensitivity to bound fluid below a 33-ms cutoff (dashed line in Fig. 5).

The sensitivity curves show the contribution to each window sum from a unit amplitude of signal having a

particular T2 relaxation time. Note that the sensitivities to fast relaxation times, of the order of a few milliseconds, can be increased (e.g., the curves in Fig. 5 shifted to the left) by using shorter early time windows. Simulations have shown, however, that using shorter early time windows provides negligible practical increases in CMR porosity and is less robust in the presence of noise. The reason for this is that only the first few echoes contain contributions from signals having relaxation times shorter than a few milliseconds.

Maximum Likelihood Estimation. The statistical properties of the window sums are used to derive a maximum likelihood function for these random variables. The amplitudes of the components in the multi-exponential relaxation model (i.e., the T2-distributions) are determined by maximizing the likelihood function subject to a constraint that the amplitudes be non-negative. The relaxation times in the relaxation model are determined by user inputs (see the section entitled ***Parameter Selection***) and are therefore not part of the estimation. This means that, except for the positivity constraint, the estimation problem is linear.

The Tikhonov regularization method is used with a minimum norm criterion to select a smooth distribution that is consistent with the raw data. Monte Carlo simulations using the minimum norm regularization criterion have shown that its use results in essentially unbiased minimum variance estimates of log outputs over the entire range of SNR. The regularization parameter is computed from the input data using an algorithm derived from a criterion that seeks to minimize the error between the computed T2-distributions and the true underlying T2-distributions. It has been shown that the resulting distributions are relatively insensitive to the value of the regularization parameter for a fairly wide range of values.[9,12] It is worth mentioning that the flexibility of the WP algorithm allows its use with other smoothing functionals including those employed in the maximum entropy method.

Connection With Eigenfunction Expansions. T2-distributions estimated from the WP algorithm are equivalent to eigenfunction expansions[12] in terms of a few orthogonal eigenfunctions (i.e., with non-zero eigenvalues). The eigenfunction analysis provides a theoretical framework for understanding the following features of the algorithm: (1) the insensitivity of the processed results to the positions of the windows and (2) why adding more windows does not change the results and (3) the relative insensitivity of the processed results to the regularization parameter.

Measurement Sensitivity Limits. The sensitivity of the NMR measurements to decay times of the order of a few milliseconds is difficult to quantify because there is no sharp cutoff on the sensitivity response to short relaxation times. This can be seen from the sensitivity plots in Fig. 5. The loss of sensitivity to short relaxation times is gradual and depends on the SNR of the measured data; however it is the inter-echo spacing that provides an intrinsic lower limit to the shortest relaxation times that can be measured. For the CMR tool, this limit is a few milliseconds. The CMR porosity reads essentially zero porosity in hard shales and contains contributions from pores with relaxation times greater than a few milliseconds. The CMR porosity is therefore an effective porosity that does not include contributions from clay-bound water. NMR laboratory measurements on core samples have shown that clay-bound waters have relaxation times below about 3 ms.[13]

Standard Deviations In Log Outputs. An important log quality control feature of the processing is the computation of the standard deviations in all of the derived log outputs. The standard deviations can be reduced, albeit with some loss of vertical resolution, by averaging of PAPs prior to processing the data. Thus, for a typical CMR sandstone logging mode, a CPMG consists of a 1.3 second wait time followed by the acquisition of 600 spin echoes. The total time for acquisition of a single PAP is 3 seconds. The three-level averaging results in total CMR porosity having a statistical precision of less than 1.0 p.u., a free-fluid porosity with a precision of less than 0.5 p.u. and a capillary bound-fluid porosity with precision of about 1.0 p.u.

Monte Carlo simulations have shown that the statistical precisions quoted above will vary slightly depending on the characteristics of the underlying T2-distributions. The porosity precision is comparable to that obtainable with nuclear logging tools. An important difference, however, is that the CMR porosity standard deviations are essentially independent of the SNR of the measurements (i.e., do not depend on the porosity of the formation), whereas the precisions of measurements made by nuclear logging tools are known to vary with porosity.

Unlike the CMR porosity measurements, the standard deviations in the logarithmic mean relaxation times depend on the SNR of the measurements. Therefore, an absolute precision specification cannot be quoted for the estimated logarithmic mean relaxation times. The computed standard deviations in the mean T2 are output on a quality control log.

The standard deviations in the logs are computed from a covariance matrix for each measurement. The computations require an estimate of the RMS noise. As noted earlier, the RMS noise is estimated from the data in a noise channel that is computed for each measurement. Fig. 6 shows the noise channel for the spin echoes in Fig. 1.

Parameter Selection. The computation of T2-distributions and log outputs requires the selection of a set of processing parameters: (1) the number of components in the multi-exponential relaxation model (or equivalently the number of points on the continuous T2-distribution), (2) the minimum and maximum values of T2 in the computed T2-distribution, (3) the free-fluid cutoff, (4) an input T1/T2

ratio and (5) the mud filtrate relaxation time. These parameters are inputs for the computation of T2-distributions, relative amounts of free- and bound-fluid porosity and mean relaxation times. It is useful to briefly discuss and define the role played by each of these parameters.

Number of Components. An input to the processing is the number of components in the multi-exponential model. Simulations and processing of field data have shown that the number of components has negligible effects on the CMR log outputs (which are integrals of the T2-distribution) provided that at least a 10-component model is employed. Adding more components results in having more points on the computed T2-distributions and is necessary for displaying continuous T2-distributions. During depth logging, a 30-component model is frequently used so that T2-distributions can be displayed while logging. For station logging, a 50-component model is normally employed.

T2min and T2max. The minimum and maximum T2 values specify the range of the T2-distribution assumed in the relaxation model. Specification of T2min, T2max and the number of components determines the relaxation times in the model, which are chosen equally spaced on a logarithmic scale. The minimum value of T2 is determined by the intrinsic sensitivity limit of the measurement to short relaxation times. The intrinsic limit for a measurement is set by the inter-echo spacing. The CMR pulse sequences, under normal conditions, have an inter-echo spacing of 0.32 ms. This suggests that the minimum T2 should be set in the range from 1 to 3 ms. The choice is not critical since, for practical purposes, the log outputs are relatively insensitive to T2min. However, using 3 ms provides slightly improved porosity precision.

The value of T2max that is selected for processing is a compromise between the longest relaxation time that can be present in the T2-distribution and the longest relaxation times that can be resolved by the measurement. The latter is determined by the echo collection time, i.e., the number of spin echoes in the CPMG and the inter-echo spacing. Simulations have shown that CMR log outputs are insensitive to the value of T2max over a reasonable range of values. For CMR depth logging with 600 or 1200 echoes, a value of 3000 ms is typically used for T2max. Re-processing of depth log data using values of T2max in the range from approximately 1500 to 3500 ms should produce negligible practical changes in the logs.

During station logging, 3000 to 8000 echoes are usually collected and a value of 5000 ms for T2max is typically used. Station logs with long echo collection times are required to resolve features in T2-distributions corresponding to relaxation times of the order a few seconds. Simulations and field data have shown, however, that long echo collection times are not required to determine accurate values of the CMR log outputs. That is, values of ϕ_{cmr}, ϕ_{ff}, ϕ_{bf} and $T_{2,log}$ obtained during depth logging will agree to within statistical uncertainties with station log outputs.

Free-fluid Cutoff. The free-fluid cutoff is an input parameter that is used to partition ϕ_{cmr} into free- and bound-fluid porosity. The cutoff depends on lithology, and cutoffs have been determined empirically for some sandstones and carbonates.[2,13] The experimental data support a value of 33 ms in sandstones and 100 ms in carbonates. The cutoff is defined so that ϕ_{ff} represents the CMR porosity associated with relaxation times greater than or equal to the cutoff. It should be noted that the quoted cutoffs for sandstones and carbonates are not expected to be universally applicable.

T1/T2 Ratios. The T1/T2 ratio is a parameter used to make a polarization correction. The correction accounts for the incomplete polarization of the proton magnetization during the wait time that initiates a CMPG. The correction is important in rocks having T1-distributions with long relaxation times as explained below.

The rate at which the proton magnetization approaches its equilibrium value depends on the T1-distribution of longitudinal relaxation times in the sample. If the wait time is too short, the signal associated with the longer relaxation times will be reduced (e.g., ϕ_{ff} will be too low). Ideally, the wait time should be at least three times the longest relaxation time in the T1-distribution. In some logging environments (e.g., vuggy carbonates) this would require wait times longer than 10 seconds, which is clearly not practical for logging measurements.

Laboratory experiments,[6] on a lithologically mixed suite of water-saturated rocks, have shown that: (1) T1 and T2-distributions have approximately the same size and shape and (2) T1/T2 ratios range from approximately 1 to 3 with a mean of about 1.65. The experiments were performed, and are valid, in the 2-MHz frequency range of the CMR tool. An inter-echo spacing of 0.32 ms was used in acquiring the experimental data. At higher frequencies and for longer inter-echo spacings, the results are not necessarily valid.

Moreover, the experimental findings are valid only in the absence of molecular diffusion effects. Under normal circumstances the CMR tool response is not affected by diffusion. An exception occurs in zones with unflushed gas. The relatively large gas diffusion constant can cause diffusion effects that reduce the T2 of the gas. Since T1 is not affected by diffusion, enhanced T1/T2 ratios are possible.

T1/T2 ratios can be logged by the CMR tool using multi-wait time CPMG pulse sequences. Multi-wait time pulse sequences are presently available for CMR station logging and a depth logging multi-wait time pulse sequence is being tested.

The CMR polarization correction for single wait time logging uses an assumed input value for the T1/T2 ratio (e.g., a value near the experimental mean of 1.65). The correction is more important for short wait times. Using longer wait times reduces not only the magnitude of the correction but also any errors in log outputs that occur because the assumed ratio is not equal to the actual T1/T2 ratios. Note that if the assumed T1/T2 ratio is greater than the actual ratio in the formation, then ϕ_{ff} will be overestimated; the converse is also true.

Mud Filtrate Relaxation Time. The mud filtrate relaxation time should be measured by the logging engineer at the wellsite prior to logging operations. The filtrate relaxation times in mud systems containing paramagnetic ions (e.g., Cr^{++}) or ferromagnetic (e.g., iron) contaminants from the drilling process can be less than 100 ms. In such environments, mud filtrate that invades the formation can suppress the long relaxation components in the T2-distributions. If a correction is not applied, then ϕ_{ff}, ϕ_{bf} and $T_{2,log}$ might not be accurate. The CMR porosity is not affected by the filtrate relaxation time; however, if a correction is not applied, then the permeability estimator based on $T_{2,log}$ can be pessimistic. It should be noted that, in practice, mud filtrate relaxation times of the order of 1 s are frequently encountered and the correction is negligible.

Calibration and Environmental Corrections. The computation of ϕ_{cmr}, ϕ_{ff}, and ϕ_{bf} requires additional environmental and calibration parameters. These include the master calibration constant, the formation temperature, the magnetic field strength and the hydrogen index of the fluids in the zone of investigation of the measurement.

Calibration Constant. Master calibrations are performed in the shop at regular intervals. The master calibration is used to convert signal amplitudes obtained in the borehole into porosity units. During the master calibration, a fixture containing a water sample is placed on the tool antenna cover. The fixture was designed so that the water completely fills the sensitive region of the measurement. The water is doped with Nickel Chloride [NiCl] to reduce the water relaxation time to approximately 50 ms. This allows the use of a short wait time and consequently a fast calibration; excellent SNR is achieved by averaging the data over a 5-minute period.

The spin-echo data are processed to determine the signal amplitude from the water solution. This signal amplitude represents a 100 p.u. standard. During logging, the CMR porosity is simply the ratio of the signal amplitude determined downhole to the master calibration amplitude. Temperature and magnetic field strength corrections are applied to this calibrated porosity to obtain an environmentally corrected CMR porosity. A hydrogen index correction may also be applied.

The master calibration signal amplitude is stored in firmware located in the tool, together with the magnetic field strength and temperature during the calibration.

Temperature Correction. As noted earlier, signal amplitudes measured in boreholes must be corrected for the Curie law effect that causes a reduction in signal amplitude with temperature. The formation temperature is used in the correction together with the master calibration temperature (i.e., the temperature that corresponds to the 100 p.u. signal). The formation temperature is derived from a temperature sensor located in the tool.

Magnetic Field Strength. The amplitude of the measurement is proportional to the square of the magnetic field strength in the zone of investigation. The field strength changes with tool temperature and, therefore, a correction is applied to account for the fact that the master calibration is performed at a different field strength.

In practice, other effects besides temperature can cause changes in the magnitude of the static field. Iron scrapings from the drilling process can adhere to the tool magnets and perturb the static field. The CMR tool has a special pulse sequence for measuring the static field strength downhole that is used immediately prior to logging. During logging, the field strength is estimated from a Hall probe and temperature sensor located in the sonde and the correction is automatically applied.

Hydrogen Index. The hydrogen index of the fluid in the zone of investigation of the measurement is an input parameter used by the processing. It is used to correct for the fact that the tool master calibration is performed using a water sample with a hydrogen index of 1. The software computes the hydrogen index of formation fluids from the measured salinity of a mud filtrate sample, the formation temperature and formation pressure. This correction is an option in the wellsite software.

The hydrogen index correction assumes that the formation fluids are mud filtrate and is therefore an approximation. However, it is an important correction in saline muds. For example, if the mud filtrate has a hydrogen index of 0.95, ϕ_{cmr} will be 5% too low if the correction is not applied. In zones with unflushed hydrocarbons, the hydrogen index of the composite fluids is generally unknown. It depends on many variables including the fluid saturations, formation pressure, oil properties, and gas types (methane, propane, etc.). The effects of gas and other hydrocarbon fluids on the responses of NMR tools are areas of ongoing investigations. The gas effect on the CMR tool is analogous to the gas effect on neutron logging tools, and results in reduced values of ϕ_{cmr}.

Simulations

In this section, the results of three Monte Carlo computer simulations are discussed. The simulations are the equivalent of "computer experiments" and are used here to elucidate: (1) the accuracy and precision of CMR log outputs, (2) the nature of the statistical fluctuations that occur on the computed T2-distributions and, in particular, (3) the CMR responses in typical clean sand, shaly sand and carbonate formations.

The use of simulated data is valuable for testing and evaluation of signal processing algorithms since the results of the simulations can be compared to the known inputs. Of course, with field or lab data, such comparisons are not possible because the true (i.e., input) values are unknown.

Before a discussion of simulation results, however, it is useful to describe how the Monte Carlo simulations are performed. An input T2-distribution is used together with the NMR measurement kernels to generate a noise-free, spin-echo sequence. Zero mean Gaussian noise is then added to each echo in the sequence. For the simulations presented in this paper, the RMS noise amplitude is 2 p.u., a value that is realistic for CMR depth logging with three-level averaging. This process is repeated 100 times, using different realizations of the random noise, to generate 100 spin-echo sequences.

The resulting spin-echo sequences are then processed using parameter values that are identical to those used to process field depth logs. The resulting log outputs represent a sample drawn from a statistical population. For a sufficiently large sample size, the statistics of the finite sample approach those of the random population. The sample statistics obtained using a sample size of 100 can be shown to provide a good approximation to the population statistics of the CMR log outputs. Therefore, the results of the simulations should represent the expected log responses in real formations having T2-distributions similar to those of the model distributions.

The computed logs for the clean sand, shaly sand and carbonate simulations are shown in Figs. 7, 8 and 9, respectively. The log presentations are similar for each simulation, i.e.,

- Vertical lines are used to show the input values.
- The input T2-distribution is shown below Track 3.
- The computed T2-distributions (for clarity only every other one is displayed) are shown in Track 3, together with values of $T_{2,log}$.
- The primary CMR log outputs, ϕ_{cmr} and ϕ_{ff}, are shown in Track 2.
- In Track 1, are shown ϕ_{cmr} and window porosities determined from the first two window sums. $\phi_{2,30}$, is the raw porosity from the first window sum (the average of the amplitudes from spin echoes 2 through 30) and similarly for $\phi_{31,100}$. The raw porosities are obtained, without any signal processing, by application of calibration and environmental corrections to the average spin-echo amplitudes in each window. Recall that, for the CMR tool, the first echo is affected by 90 degree ringing and is not used in the processing. The window porosities are random variables with known statistical properties. The window porosities are not routinely displayed on CMR field logs and are shown for instructional purposes.

Summary of Simulations. The inputs for each of the simulations are shown in Table 1. The sample means and their standard deviations for all of the CMR log outputs are shown in Table 2. The "expected" CMR responses in Table 2 are equal to the inputs for the T2-distributions, used in the simulations, if relaxation times in the distributions less than 3 ms are ignored. These inputs represent ideal CMR responses assuming that there is a sharp cutoff of 3 ms for the tool sensitivity to short relaxation times. The good agreement between the expected responses and the results of the simulations lends credence to a tool sensitivity limit of about 3 ms.

The averages of the sample standard deviations of ϕ_{cmr} and ϕ_{ff} for the three simulations are 0.64 and 0.34 p.u., respectively. These values are representative of standard deviations in CMR field logs.

Accurate and precise estimates are obtained for ϕ_{ff} for all three simulations including the shaly sand. ϕ_{cmr} is equal to total porosity in the clean sand and carbonate simulations because the input distributions do not have short relaxation times. In the shaly sand, however, ϕ_{cmr} is an effective porosity and is not equal to total porosity.

The sample standard deviation of ϕ_{ff} is superior to those of ϕ_{cmr} and ϕ_{bf}. Figure 5 demonstrates why the CMR bound-fluid porosity has poorer repeatability than does the free-fluid porosity. Only a relatively few echoes have any sensitivity to the faster decaying signals that contribute to the bound-fluid.

The sample standard deviation in ϕ_{bf} is slightly higher than that computed by assuming that the errors in ϕ_{cmr} and ϕ_{ff} are independent. This assumption is incorrect since one can show that errors in free-fluid and total porosity are statistically correlated.

Clean Sand Simulation. The input distribution shown in Fig. 7 for the clean sand simulation has its dominant signal amplitudes in the mid T2 range; i.e., from 10 to 200 ms and has negligible (e.g., 0.3 p.u.) porosity with relaxation times below 3 ms. The absence of both fast and

long components make this a comparatively simple environment for CMR logging. The simulations were performed with sequences consisting of 600 spin-echo amplitudes with an echo spacing of 0.32 ms. A T2 cutoff of 33 ms was used to compute the free-fluid porosity. These values are typically used for CMR logging in sandstone reservoirs.

The input values of total porosity, free-fluid porosity, bound-fluid porosity and logarithmic mean relaxation time are 15.0, 10.5, 4.5 p.u. and 44 ms, respectively.

Although the overall shapes of the computed T2-distributions in Fig. 7 are qualitatively similar to each other and to the input distribution, there are small differences. These differences are artifacts due to statistical fluctuations. Although the fluctuation effects can be reduced by reducing the RMS noise, it is not possible to totally eliminate these effects. The T2-distributions shown in Fig. 7 clearly show that caution should be used in interpreting small details on logs of computed T2-distributions.

The mean of the 100 samples of $\phi_{2,30}$ shown in Fig. 7 is 12.7 p.u. with a standard deviation of 0.39 p.u. ϕ_{cmr} agrees well (sample mean of 14.9 p.u.) with the total porosity (15.0 p.u.) whereas $\phi_{2,30}$ is more than 2.0 p.u. lower than the input porosity. This can be understood from the sensitivity plots shown in Fig. 5. $\phi_{2,30}$ has reduced sensitivity to fast relaxation times and therefore would not be a good porosity estimator.

Shaly Sand Simulation. The input distribution shown in Fig. 8 for this simulation has significant signal amplitude at short T2 values. For these types of distributions, ϕ_{cmr} underestimates total porosity due to insensitivity to fast components. The intrinsic insensitivity of NMR data to fast decays is due to finite inter-echo spacing and the fact that only the first few echoes contain information on the shortest relaxation times.

The input values of total porosity, free-fluid porosity, bound-fluid porosity and logarithmic mean relaxation time are 15.0, 2.7, 12.3 p.u. and 8.4 ms, respectively.

The sample mean of the ϕ_{cmr} values shown in Fig. 8 is equal to 11.4 p.u. The input T2-distribution has 3.6 p.u. of porosity with relaxation times less than 3 ms; hence, the CMR porosity can be roughly correlated with a 3-ms sensitivity cutoff. Components below 3 ms are associated with clay-bound waters and microporosity in shales.[13] For this reason, ϕ_{cmr} is considered to be an "effective porosity."

The sample mean of the $T_{2,log}$ values shown in Fig. 8 is equal to 16.5 ms compared to an input value of 8.4 ms. The overestimation of the input mean relaxation time is a direct consequence of the measurement insensitivity to clay-bound water; however, the sample mean is in excellent agreement with the expected mean relaxation time of 15.8 ms arrived at by assuming that the tool is insensitive to relaxation times below 3 ms.

The good agreement between ϕ_{cmr} and $\phi_{2,5}$, shown in Track 1, indicates that both have similar sensitivities to fast components. In principle, echo number 2 could be used as a porosity estimator. This porosity would read closer to the input total porosity but would have poor precision, e.g., a standard deviation of 2 p.u. assuming three-level averaging. To achieve precision comparable to ϕ_{cmr}, twelve-level averaging would be required, which would degrade the vertical resolution of the log.

Carbonate Simulation. T2-distributions in typical carbonate rocks are characterized by long relaxation times. To resolve these components, it is necessary to acquire a larger number of echoes than for sandstones. For CMR depth logging, 1200 echoes are usually collected compared to 600 in sandstones.

The input values of total porosity, free-fluid porosity, bound-fluid porosity and logarithmic mean relaxation time are 20.0, 17.7, 2.3 p.u. and 258 ms, respectively. A free-fluid cutoff of 100 ms is used to compute free-fluid porosity. The sample mean of the ϕ_{cmr} values shown in Fig. 9 is equal to 20.2 p.u.

Field Data

CMR Log Responses. A log over a 200-ft [61-m] interval from a well drilled in a sandstone formation is shown in Fig. 10. Gamma ray and caliper logs are displayed in Track 1. Logs of $T_{2,log}$ and permeability are displayed in Track 2. The permeability log was computed from ϕ_{cmr} and $T_{2,log}$ using an empirical relationship.[2] Logs of ϕ_{cmr}, ϕ_{ff}, neutron, and density porosity are displayed in Track 3. The shading between the ϕ_{cmr} and ϕ_{ff} curves is used to show ϕ_{bf}. The T2-distributions are displayed in Track 4. All the logs shown can be displayed in real time at the wellsite.

The interval, shown in Fig. 10, contains a 10-ft [3-m] thick upper zone that is typical of a clean sand (marked CS on the log). In this zone, ϕ_{cmr} and the density log porosity are in good agreement. The T2-distributions are indicative of a clean permeable sand with almost all of ϕ_{cmr} derived from relaxation times greater than about 10 ms. The $T_{2,log}$ and permeability logs also indicate a clean permeable sand with predominantly large pores. About 80% of the porosity in the clean sand is free-fluid porosity, the remaining 20% is capillary bound-fluid porosity.

Below the clean sand is a long, shaly sand interval that is bounded from below by a gas sand (marked GS on the log). The large separation of the neutron/density logs in this interval is indicative of its shaliness and the high neutron readings are indicative of clay-bound water. Observe that, as discussed previously, ϕ_{cmr} is an effective porosity and

reads less than the density (total) porosity in shaly sands. In general, note that the separation between ϕ_{cmr} and density porosity increases in zones with higher neutron porosity (e.g., more clay-bound water). The short relaxation times are evident on the T2-distributions and the $T_{2,log}$ curve. As expected, the shaly zones have negligible free-fluid porosity. These observations are confirmed by the permeability log reading less than 1 md over most of the interval.

The zone at the bottom of the interval (marked GS) shows the CMR log response in a zone containing unflushed gas. The gas effect in this interval is indicated by neutron/density crossover. The reduced hydrogen index of the gas causes ϕ_{cmr} to read too low. A gas correction to ϕ_{cmr} can be made but it requires knowledge of the fluid types and saturations in the zone of investigation.

Log Repeatability. The excellent repeatability of the primary CMR log outputs ϕ_{cmr}, ϕ_{ff}, and $T_{2,log}$ over the lower 100 ft [30 m] of the interval is shown in Fig. 11. The logs were acquired at 600 ft/hour [183 m/hour] using a typical CMR depth logging sequence with three-level averaging.

Conclusions

Using Monte Carlo simulations and field data, we have demonstrated that the CMR tool signal processing software provides accurate and precise high-resolution logs of effective porosity, free-fluid porosity, and capillary bound-fluid porosity. Logs of T2-distributions, mean relaxation times, and permeability are also provided at the wellsite. CMR logs provide continuous quantitative information on producibile fluids and pore size distributions that was previously obtainable only over limited intervals by more expensive coring and well testing operations.

In typical clean sands and carbonates, the CMR porosity is equal to total porosity. In shaly sands, the CMR porosity does not include porosity associated with clay-bound water and therefore is an effective porosity. More specifically, CMR porosity is insensitive to microporosity having relaxation times less than a few milliseconds.

Standard deviations of less than 0.8 p.u. in CMR porosity, less than 0.5 p.u. in free-fluid porosity, and less than 1.0 p.u. in capillary bound-fluid porosity results in CMR logs with precisions comparable to neutron/density logs.

Ackowledgments

We thank the management of Schlumberger for permission to publish this paper. A debt of gratitude is owed to the CMR tool engineering and research teams and the Schlumberger field organization for making this work possible.

Nomenclature

ϕ_{cmr} = CMR porosity, p.u.

ϕ_{ff} = CMR free-fluid porosity, p.u.

ϕ_{bf} = CMR capillary bound-fluid porosity, p.u.

$T_{2,log}$ = CMR logarithmic mean relaxation time, ms

$\phi_{m,n}$ = window porosity from echoes m through n, p.u.

References

1. Farrar, T.C. and Becker, E.D.: *Pulse and Fourier Transform NMR*, Academic Press, 1971.
2. Morriss, C.E., et al.: "Field Test of an Experimental Pulsed Nuclear Magnetism Tool," *Trans.* SPWLA 34th Ann. Logging Symp., Calgary, June 13-16, 1993, Paper GGG.
3. Chandler, R., et. al.: "Improved Log Quality With a Dual-Frequency Pulsed NMR Tool," paper SPE 28365 presented at the 1994 SPE Annual Technical Conference and Exhibition, New Orleans, Sept. 25-28.
4. Kleinberg, R.L., et. al.: "Novel NMR Apparatus for Investigating an External Sample," J. of Mag. Resonance (1992), **97**, 466-485.
5. Gallegos, D.P. and Smith, D.M.: "A NMR Technique for the Analysis of Pore Structure: Determination of Continuous Pore Size Distributions," J. of Colloid and Interface Science (1988), **122**, No. 1, 143-153.
6. Kleinberg, R.L., et al.: " Nuclear Magnetic Resonance of Rocks: T1 vs. T2," paper SPE 26470 presented at the 1993 SPE Annual Technical Conference and Exhibition, Houston, Oct. 3-6.
7. Tikhonov, A.N. and Arsenin, V.Y.: *Solution of Ill-Posed Problems*, V. H. Winston and Sons, 1977.
8. Twomey, S.: *Introduction to the Mathematics of Inversion in Remote Sensing and Indirect Measurements*, Elsevier Scientific Publishing Co., 1977.
9. Freedman, R.: "Processing Method and Apparatus For Processing Spin-Echo In-Phase and Quadrature Amplitudes From a Pulsed Nuclear Magnetism Tool and Producing New Output Data To Be Recorded On An Output Record," U.S. Patent No. 5,291,137, (1994).
10. Freedman, R.: "Method and Apparatus For Compressing Data Produced From A Well Tool In A Wellbore Prior To Transmitting The Compressed Data Uphole To A Surface Apparatus," U.S. Patent No. 5,381,092, (1995).
11. Daubechies, I.: "The Wavelet Transform, Time-Frequency Localization and Signal Analysis," IEEE *Trans.* Information Theory (1990), **36**, 961-1005.
12. Chung, W.: "Inversion of Pulsed NMR Data Using Eigenanalysis," M.S. thesis, Mass. Institute of Tech., May 1993.
13. Straley, C., et al.: "Core Analysis by Low Field NMR," *Proc.*, 1994 Int. Symp. of the Soc. of Core Analysts, Stavanger, Norway, Sept. 12-14, 43-56.

Table 1- Simulation Inputs			
Input	**Clean Sand**	**Shaly Sand**	**Carbonate**
Total Porosity	15.0 p.u.	15.0 p.u.	20.0 p.u.
Free-fluid Porosity	10.5 p.u.	2.7 p.u.	17.7 p.u.
Bound-fluid Porosity	4.5 p.u.	12.3 p.u.	2.3 p.u.
Mean Relaxation Time	44.0 ms	8.4 ms	258 ms

Table 2- Simulation Summary						
Output	**Clean Sand**		**Shaly Sand**		**Carbonate**	
	Expected*	Simulation	Expected*	Simulation	Expected*	Simulation
ϕ_{cmr}	14.7	14.9 ± 0.80	11.4	11.4±0.65	20.0	20.2±0.48
ϕ_{ff}	10.5	10.2±0.42	2.7	2.9±0.24	17.7	17.5±0.36
ϕ_{bf}	4.2	4.7±1.0	8.7	8.5±0.76	2.3	2.7±0.56
$T_{2,log}$	46.4	46.8± 6.0	15.8	16.5±1.4	258	256±23
$\phi_{2,5}$	NA	14.3±0.98	NA	11.9±0.95	NA	19.4±1.0

* The expected CMR outputs were computed from the model input T2-distributions by ignoring relaxation times less than 3.0 ms, i.e., by assuming that the tool sensitivity to short relaxation times has a sharp cutoff at 3.0 ms.

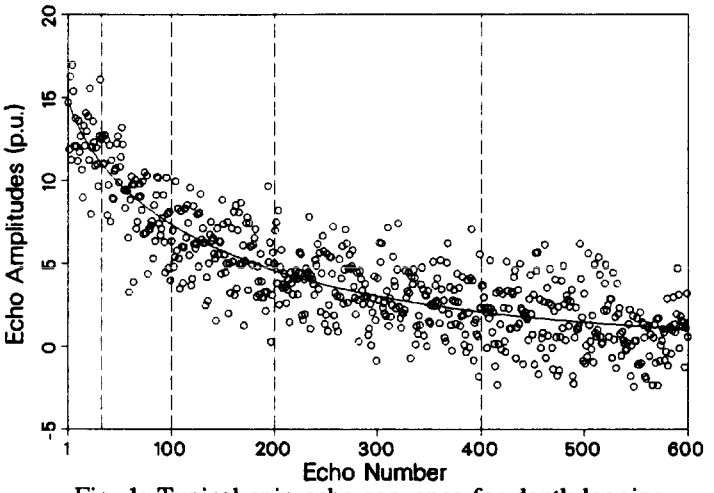

Fig. 1: Typical spin-echo sequence for depth logging. The dashed lines are window boundaries.

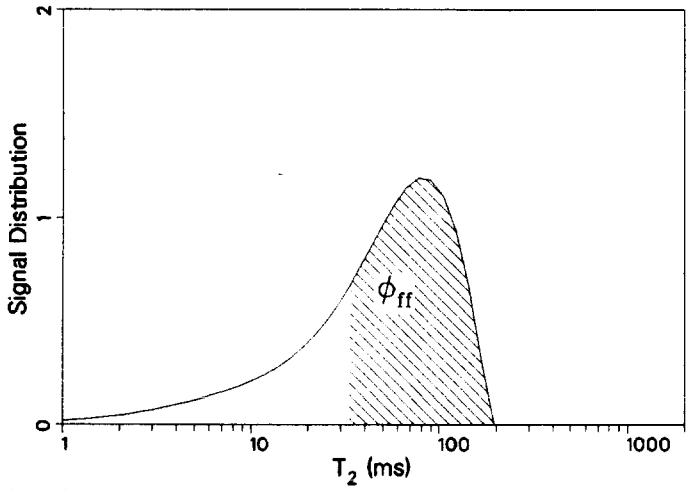

Fig. 2: Typical T2-distribution for a clean sand.

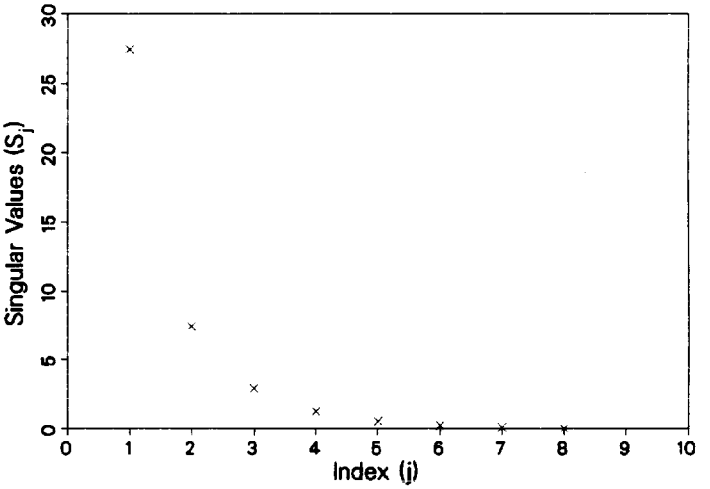

Fig. 3: The first 8 singular values of the NMR measurement kernel matrix for a typical pulse sequence with 600 spin-echoes.

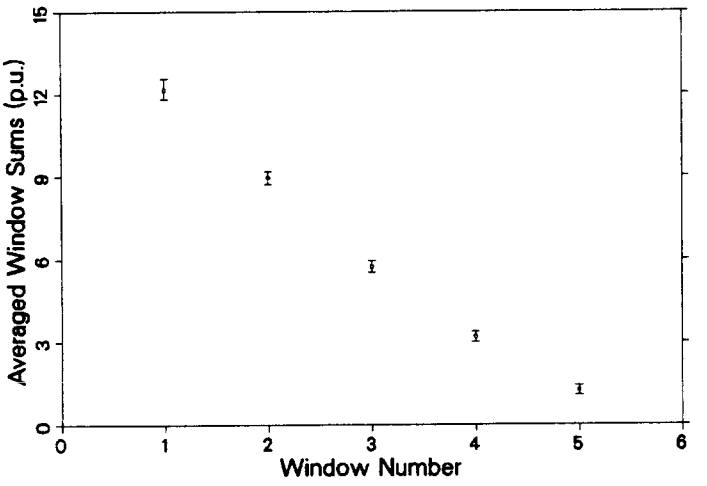

Fig. 4: Compressed data (i.e., window porosities) for the 600 spin echoes shown in Fig. 1.

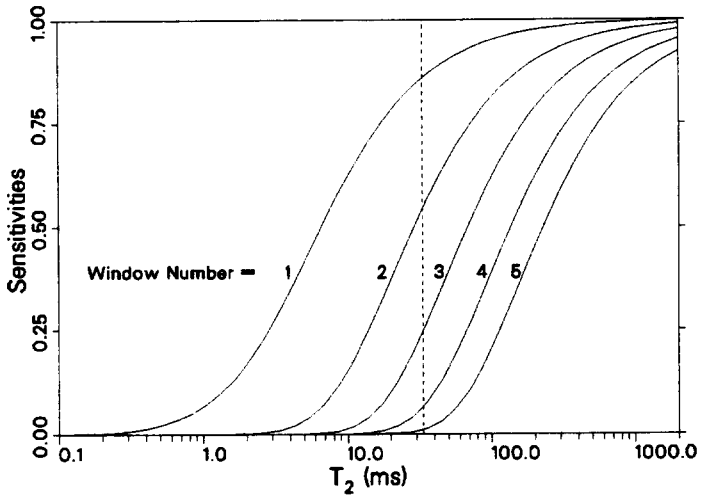

Fig. 5: Sensitivity curves for the average window sums computed using the windows shown in Fig. 1.

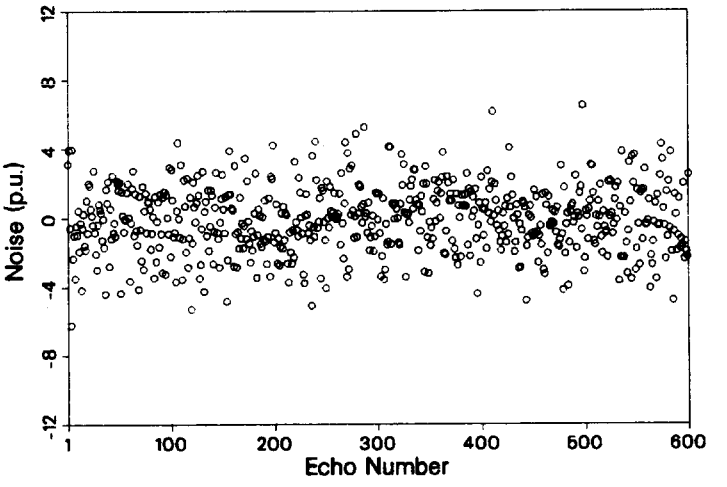

Fig. 6: Noise channel for the data shown in Fig. 1.

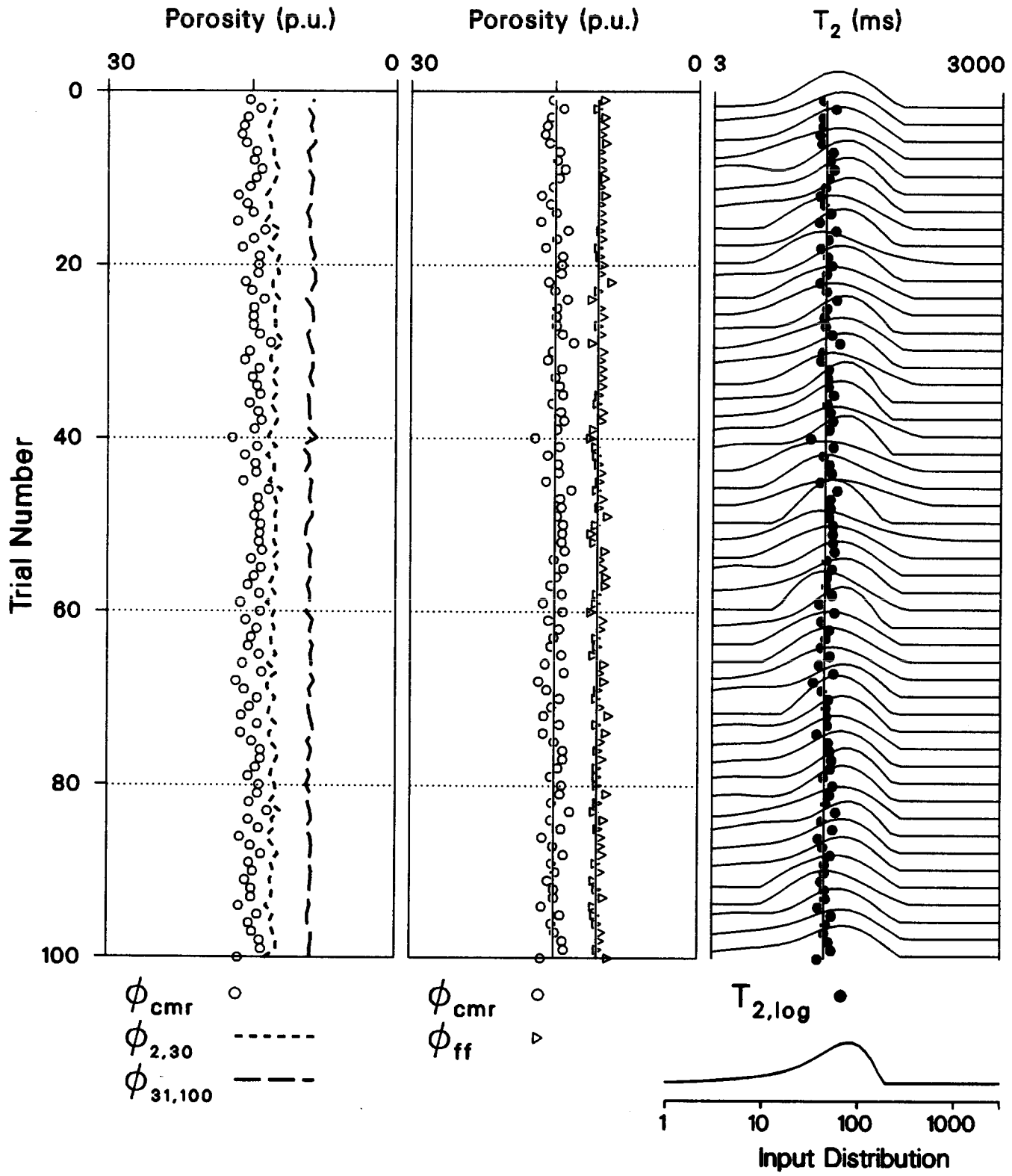

Fig. 7: The outputs of CMR processing for 100 Monte Carlo trials using spin-echo sequences computed from the input T2-distribution for a typical clean sand. ϕ_{cmr} shown by the circles in Track 2 is an accurate estimate of total porosity shown by the vertical line. In clean sands, ϕ_{cmr} and total porosity are equal. ϕ_{ff} shown by the triangles in Track 2 and $T_{2,log}$ shown by the black circles in Track 3 are also accurately estimated (agree well with the input values shown by vertical lines). ϕ_{cmr} and the first two window porosities, $\phi_{2,30}$ and $\phi_{31,100}$, are shown in Track 1. As discussed in the text, $\phi_{2,30}$ has excellent precision but underestimates ϕ_{cmr}.

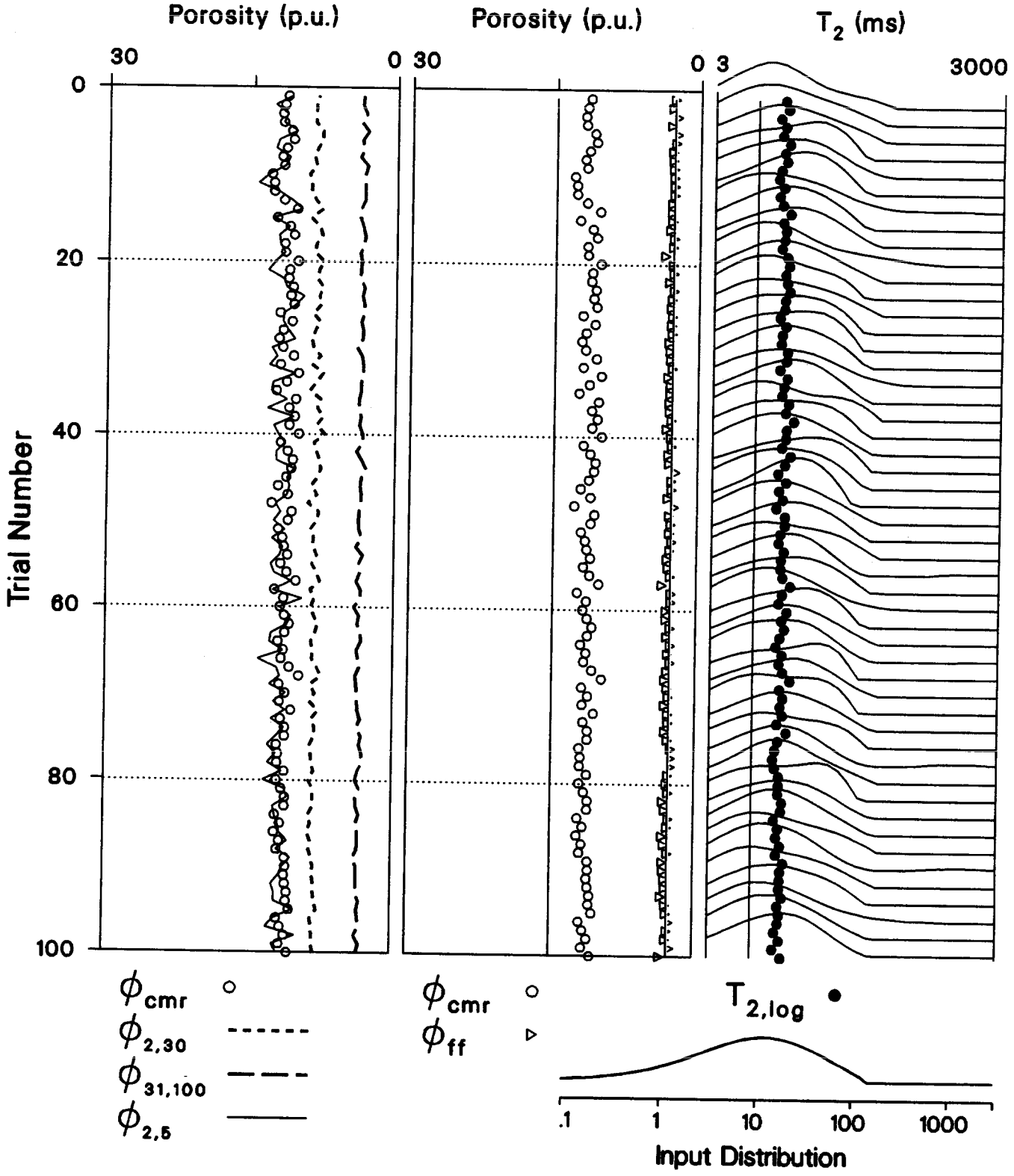

Fig. 8: The outputs of CMR processing for 100 Monte Carlo trials using spin-echo sequences computed from the input T2-distribution for a typical shaly sand. ϕ_{cmr} shown by the circles in Track 2 is an effective porosity that is not equal to total porosity (vertical line) in shaly sands. ϕ_{cmr} does not include clay-bound water and microporosity with relaxation times less than about 3 ms. ϕ_{ff} shown by the triangles in Track 2 agrees well with the input free-fluid porosity (vertical line) in shaly sands. $T_{2,log}$ shown by the black circles in Track 3 overestimates the input value (vertical line). ϕ_{cmr} and $T_{2,log}$ agree well with the expected values assuming a cutoff of 3 ms for the tool measurement sensitivity (e.g., see Table 2). ϕ_{cmr} and $\phi_{2,5}$ are comparable as shown in Track 1.

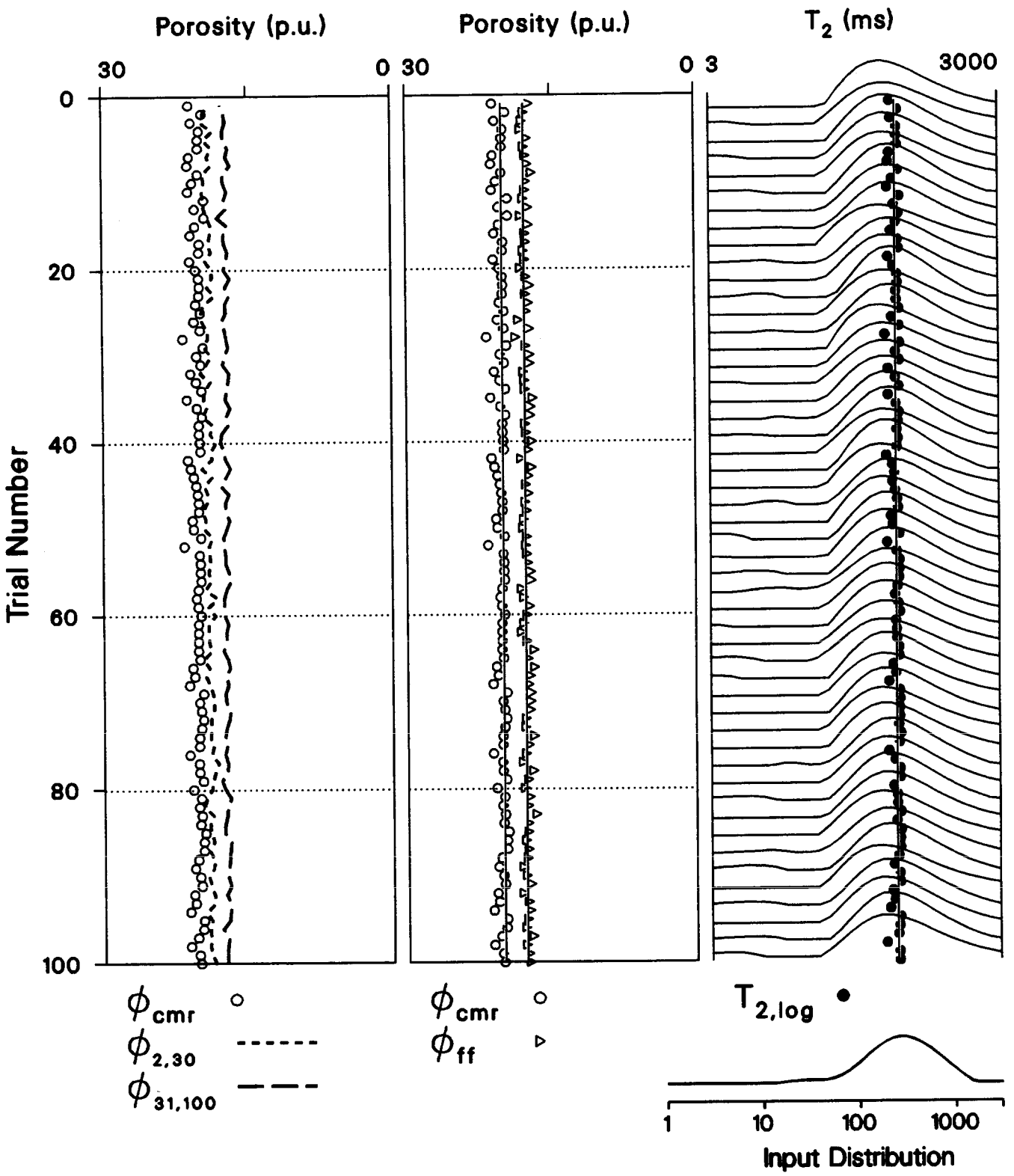

Fig. 9: The outputs of CMR processing for 100 Monte Carlo trials using spin-echo sequences computed from the input T2-distribution for a typical carbonate. ϕ_{cmr} shown by the circles in Track 2 is an accurate estimate of total porosity shown by the vertical line. In typical carbonates, ϕ_{cmr} and total porosity are equal. ϕ_{ff} shown by the triangles in Track 2, and $T_{2,log}$ shown by the black circles in Track 3 are also accurately estimated (agree well with the input values shown by vertical lines). ϕ_{cmr} and the first two window porosities, $\phi_{2,30}$ and $\phi_{31,100}$, are shown in Track 1. As discussed in the text, $\phi_{2,30}$ has excellent precision but underestimates ϕ_{cmr}.

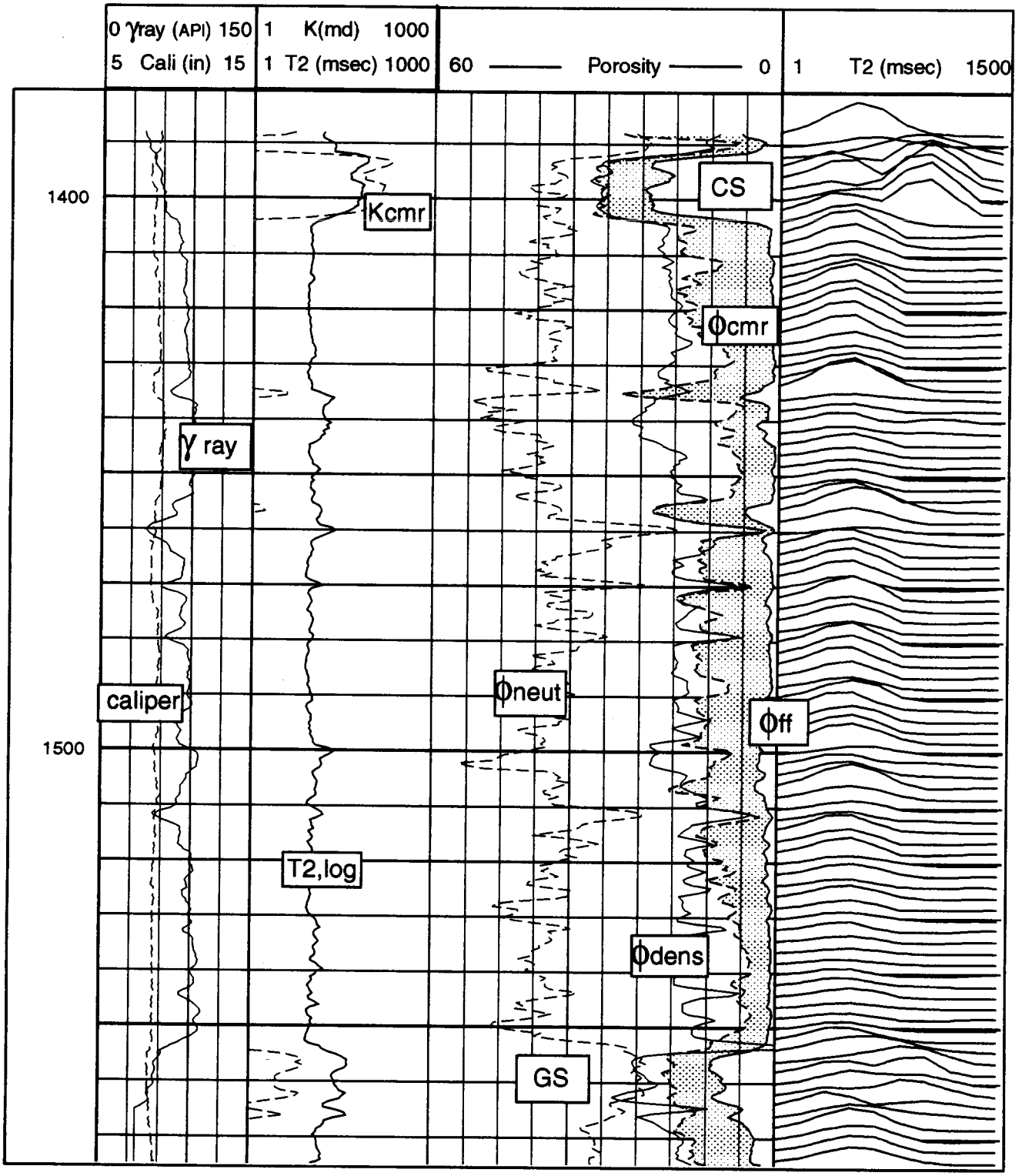

Fig. 10: CMR and neutron/density logs over a 200-ft shaly sand interval. ϕ_{cmr}, ϕ_{ff}, and neutron/density logs are shown in Track 3. $T_{2,log}$ and permeability logs are shown in Track 2. T2-distributions are shown in Track 4. ϕ_{cmr} and the density log porosity agree well in the clean sand marked CS. In the shaly section below the clean sand, ϕ_{cmr} does not include the clay-bound water porosity and therefore reads less than density porosity. The gas effect on ϕ_{cmr} is shown in the sand marked GS near the bottom of the interval. The shading in Track 3 indicates capillary-bound fluid porosity.

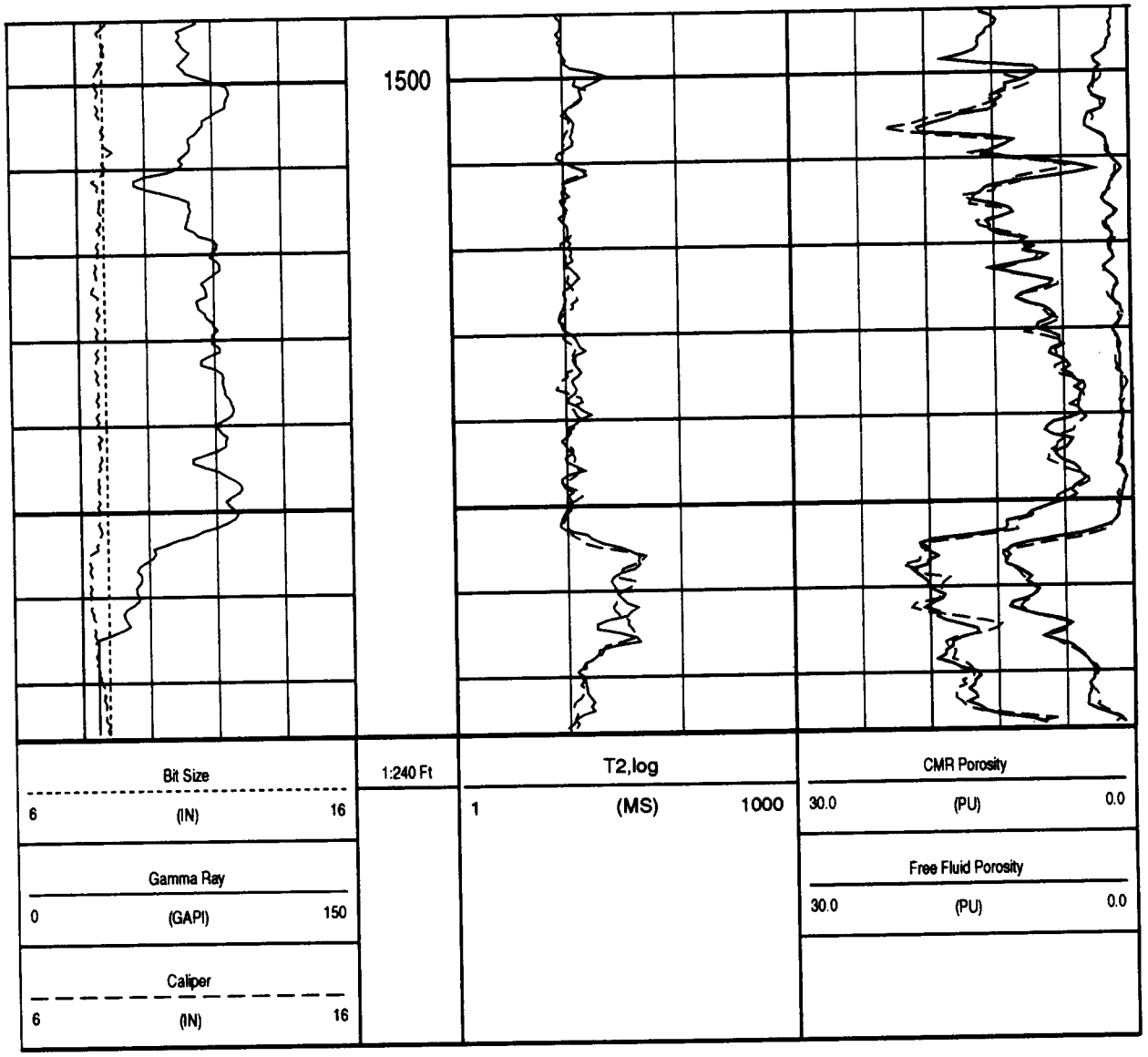

Fig. 11: Repeatability of the CMR log outputs over the lower part of the shaly sand zone shown in Fig. 10. The main log and the repeat log were both logged at 600 ft/hour using three level averaging.